Film thickness in a ball-on-disc contact lubricated with greases, bleed oils and base oils

T. Cousseau, M. Bjo¨rling, B. Grac-a, A. Campos, J. Seabra, R. Larsson

ABSTRACT

Three different lubricating greases and their bleed and base oils were compared in terms of film thickness in a ball-on-disc test rig through optical interferometry. The theoretical values calculated according to Hamrock's equation are in close agreement with the base oil film thickness measurements, which validates the selected experimental methodology.

The grease and bleed oil film thickness under fully flooded lubrication conditions presented quite similar behaviour and levels. Therefore, the grease film thickness under full film conditions might be predicted using their bleed oil properties, namely the viscosity and pressure-viscosity coefficient. Thebase and bleed oil lubricant parameter *LP* are proportional to the measured film thickness.

A relationship between grease and the corresponding bleed oil film thickness was evidenced.

Keywords: Grease, Bleed oil, Base oil, EHD optical interferometry

1. Introduction

Grease is by far the most common type of lubricant in rolling bearings. However, the lubrication mechanisms needed to predict grease behaviour in many different applications are not yet fully understood. A very interesting overview on grease lubrication in rolling bearings was published by Lugt in 2009 [1].

Several experimental investigations have been carried out to study grease film formation in concentrated contacts, such as those found in rolling bearings. Booser and Wilcock [2] postulated that rolling bearings are lubricated by the base oil released by the grease during operation. Wikstro¨ m and Ho¨ glund [3] performed full rolling bearing tests using both grease and base oil, which showed similar bearing friction torque, and claimed that these tests confirm the theory of Booser and Wilcock. In a recent study, Cousseau [4] performed full rolling bearings tests, lubricated with different greases and their corresponding base oils, and measured the rolling bearing friction torque for wide ranges of the operating conditions, showing that grease and base oil generate significantly different friction torque values. These results contradict the findings presented by Wikstro¨ m and Ho¨ glund [3], but they are in close agreement with the latest SKF rolling bearing friction torque model [5], which was validated by an extensive experimental program.

Other experimental studies with lubricating greases may be found in [6–10]. All these research works suggest the same grease film formation mechanism: initially grease builds-up a higher film thickness than its base oil, but it decreases with time and reaches a starved condition. Until now, no general theory or numerical model has been proposed to predict this film thickness generation mechanism.

In order to understand the differences between grease and base oil lubrication, Cann et al. [10,11] performed film thickness and rheological measurements, SEM photographs and FTIR spectroscopy analysis for several greases, under fully flooded conditions. The main conclusions from this study, nowadays accepted by many researchers, were:

- Thickener layers are present on the contact surface after test;
- Greases with the same formulation give higher film thickness for higher base oil viscosities;
- Greases with the same formulation give higher film thickness for higher thickener concentration;
- The film thickness difference between grease and its base oil depends on base oil viscosity, thickener type and concentration;
- The thickener of high shear stability greases is more able to survive inside the contact, making a significant contribution to EHD film thickness.

Based on these results, Cann [10,11] proposed a model for grease film formation, assuming that the surfaces are covered by a

thin film of thickener, generating a film composed of base oil thickened with thickener material.

Another grease lubrication model is often used, the sponge model. This mechanism assumes that the grease 'bleeds' oil, which replenishes the film in the raceway and lubricates the contact zone [12,2]. The model considers that base and bleed oils have the same characteristics.

The most recent studies indicate that the grease lubrication mechanism is dominated by oil thickened with broken/sheared thickener. Most likely it is similar to the product obtained through the static bleed oil test IP 121 (see Section 2.3), which has rheological properties significantly different from those of the base oil [13]. To the authors' knowledge, few scientific studies have been published concerning the bleed oil properties and their influence on the tribological behaviour of the EHD contact, namely [14,15].

In this work the film thickness generated by the grease and by its bleed and base oils were measured and compared, in order to understand the role of the bleed oil in grease lubrication. The film thickness was measured on a ball-on-disc apparatus, under fully flooded conditions, for three different greases. The film thickness measurements were used to calculate the pressure coefficient values of the base and bleed oils.

2. Method and material

2.1. Experimental apparatus

The tests were performed in a WAM (Wedeven Associates machine) ball-on-disc test apparatus, model 11A. A full description of the capabilities of this machine is presented by Bjo¨rling et al. [16]. An optical device was mounted in the WAM 11A machine in order to measure the film thickness. A picture of the WAM machine is presented in Fig. 1.

The optical interferometry measurements of lubricant film thickness have already been described by several authors. Details of this technique have been reported elsewhere [17–19] and only a brief description will be given here.

The lubricated contact is formed by the reflective steel ball and the flat surface of the glass disc. The load is applied by moving the disc downwards towards the ball. The disc is mounted on a shaft driven by an electric motor. The steel ball is also controlled by an electrical motor, allowing to run the tests under rolling/sliding conditions. The glass disc is coated with a chromium semi-reflecting coating, on top of which a spacer layer of transparent silica is deposited ($CrSiO_3$).

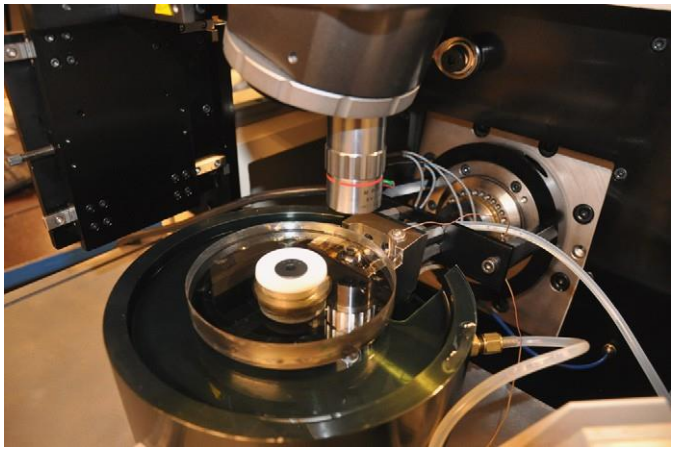

Fig. 1. View of the WAM 11A ball-on-disc test apparatus.

White light is shone through the glass disc into the contact. Part of it is reflected back by the chromium layer, while the rest passes through the silica layer and any oil film present, before being reflected back by the steel ball. Since the light has travelled different distances, upon recombination the two beams interfere optically at values of wavelength dependent on the path difference and thus the film thickness can be measured. The coloured interference image is detected by a CCD camera attached to a frame grabber, so that images could be taken from the contact region.

The method to translate the optical phase difference map into film thickness is described by several authors, see for example [19–21]. The method used here is the Lab-method described by Hartl et al. [21]. This technique is applicable also when spacer layers are used. The spacer layer imaging method allows the mapping of the film thickness with a resolution of 1 nm in the range 1 nm to 800 nm. The technique is useful for grease film thickness measurements, since the starved conditions are quickly reached and the film thickness values are in general lower than 80 nm under these conditions. With white light and without spacer layer discs it is very difficult to measure film thickness lower than 80 nm.

2.2. Test specimens

The standard ball specimen has a diameter of 13/16 in. (20.637 mm) and it is made from AISI 52100 bearing steel. The roughness of the balls was measured with a Wyko NT1100 optical profiling system from Veeco. Measurements were done using 10 x magnification and 0.5 x field of view (FOV).

The discs were made from glass which supports a maximum Hertz pressure of approximately 0.6 GPa. The silica spacer layer has a refractive index of 1.4785 according to the manufacturer.

The ball and disc properties are presented in Table 1.

2.3. Lubricants

Three lubricating greases with different formulations and their base and bleed oils were tested. The greases were named according to their chemical formulation (i.e., thickener þ base oil): LiM1 thickened with lithium and mineral base oil; LiCaE thickened with lithium and calcium and ester base oil; PPAO thickened with polypropylene, co-thickened with an elastomer and polyalphaolefin base oil. The main properties of the lubricating greases are shown in Table 2.

Ester based grease LiCaE passed the test for biodegradability (OECD 301F and SS155470 class B) and eco-toxicity (OECD 202); see Table 2.

The refractive index of the lubricants were measured using an Abbot refractometer at ambient temperature and the other lubricant characteristics were provided by the grease manufacturers.

The bleed oils of the greases were obtained according to the modified IP 121 standard test method. The IP 121 is a standard static bleed oil test, consisting of a stainless steel separation cup with a 240 mesh woven wire cloth made as a cone. Oil separation is determined by placing the grease sample on the wire mesh cone

Table 1
Ball and disc data.

	Ball	Disc
Elastic modulus—E (Gpa)	210	64
Poison coefficient—ηð=Þ	0.29	0.2
Radius—R (mm)	10.3185	50
Surface roughness—Ra (nm)	50	⁄5
Space layer thickness—(nm)	–	⁄160
Space layer refractive index—(/)	–	⁄1:4785

Table 2
Physical characteristics of the lubricant greases and of the corresponding base and bleed oils.

Designation	*LiM1*	*LiCaE*	*PPAO*
Base oil[a]	Mineral	Ester	PAO
Thickener[a]	Li	Li/Ca	Polyprop.
Biodegradability[a] (%)	–	*passed*	–
Eco-toxicity[a] (%)	–	*passed*	–
Grease properties			
NLGI number[a] (DIN 518181)	2	2	2
Dropping point[a] (1C)	185	4180	4140
Operating temperature[a] (1C)	−20=8130	−30=8120	−35=8120
Refractive index at 25 1C	1.4965	1.4837	1.4892
Bleed oil properties			
Specific gravity[a] (g/cm^3)	0.909	0.919	0.843
Viscosity at 40 1C (mm^2/s)	192.1	95.43	528.83
Viscosity at 80 1C (mm^2/s)	28.86	24.98	151.95
Refractive index at 25 1C	1.4948	1.4744	1.4639
Base oil properties			
Specific gravity (g/cm^3)	0.903	0.952	0.828
Viscosity at 40 1C (mm^2/s)	208.56	93.59	38.77
Viscosity at 80 1C (mm^2/s)	32.98	25.31	10.84
Refractive index at 25 1C	1.4956	1.4562	1.4592

[a] Provided by the grease manufacturer.

and loading it with a 100 g metal weight during 168 h at 40 1C. However, 70 1C were used to obtain sufficient amount of bleed oil to carry out rheological and film thickness measurements.

Base and bleed oil kinematic viscosities were measured in a MCR 301 rheometer with cone-plate geometry CP50-2 (2.021; 49.97 mm) at two different temperatures (40 1C and 80 1C). For that, flow tests were carried out, where increasing levels of shear rate ð10^{-2} s^{-1} o g o 10^3 s^{-1}Þ were applied to the grease's bleed and base oils while the shear stress ðtÞ and apparent viscosity ðZÞ were measured. Under these conditions, both base and bleed oil presented a Newtonian behaviour but different viscosity values. The relative viscosity difference is given by

$$\Delta\eta[\%] = \frac{\eta_{bleed} - \eta_{base}}{\eta_{base}} \times 100 \quad (1)$$

Three different trends were observed when comparing base and bleed oil viscosities at 40 1C. Grease LiCaE presented similar values for base and bleed oil viscosities. In the case of grease LiM1, the viscosity of the bleed oil is 8% lower than the viscosity of the base oil, while in the case of the grease PPAO the viscosity of the bleed oil is 1260% higher than the viscosity of the base oil. Such different behaviours are discussed in Section 3.

Scanning electron microscopy was performed on a JEOL JSM 35C/ Noran Voyager to characterize the greases (see Fig. 2). The thickener structure images show significant differences, which are related to the thickener/base oil interaction, the manufacturing process and the sample preparation. Fig. 2 shows that LiM1 thickener is a structured system, based on entanglement networks, which present long and large lithium fibres; LiCaE thickener contains several large calcium particles and the lithium fibres are shorter and thinner than in the case of LiM1. PPAO grease seems to have a more homogeneous thickener structure, although, it is easily damaged by the energy of the incident electron beam used in high magnification (20,000 x). The sample preparation, the operating conditions selected and their influence on the images obtained are discussed in [13].

2.4. Test procedure

A set of lubricant film thickness measurements was carried out with all lubricants described in Section 2.3. A scraper was used to re-distribute the grease back to the rolling track and generate fully flooded operating conditions. The load applied was 25.71 N, which corresponds to maximum Hertz pressure of P_0 ¼ 0:5 GPa. Three operating temperatures were used; 40 1C, 60 1C and 80 1C. The tests were carried out under pure rolling conditions and with a slide-to-roll ratio (SRR) of 3%. The SRR is defined by

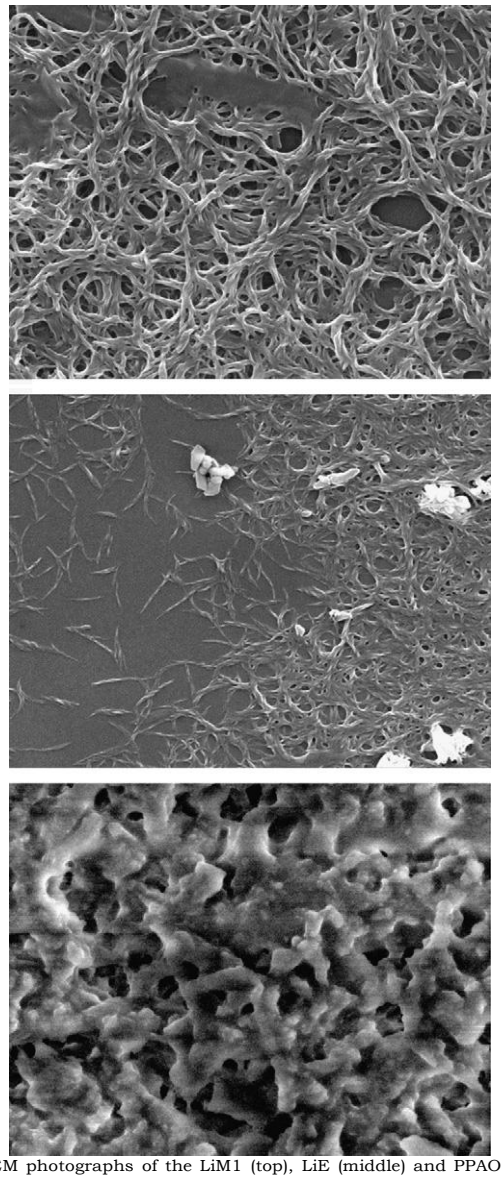

Fig. 2. SEM photographs of the LiM1 (top), LiE (middle) and PPAO (bottom); 20,000x magnification.

$$\text{ð} \quad SRR = 2 \cdot \frac{(U_{disc} - U_{ball})}{(U_{disc} + U_{ball})} \times 100\% \quad (2)$$

The entrainment speed range was different for each lubricant in order to avoid starvation. The lowest entrainment speed was selected so that a film thickness of 100 nm was measured. The highest entrainment speed was limited by two factors, the maximum measurement range of the optical device (around 800 nm—which is dependent on velocity) and the volume of lubricant available. In the case of the bleed oil, the oil amount available was not enough to keep the oil reservoir filled during the whole test. Therefore low entrainment speeds were used to avoid emptying of the oil reservoir.

In the case of the tests with greases, the operating temperature was maintained by enclosing the ball-on-disc device with a plastic

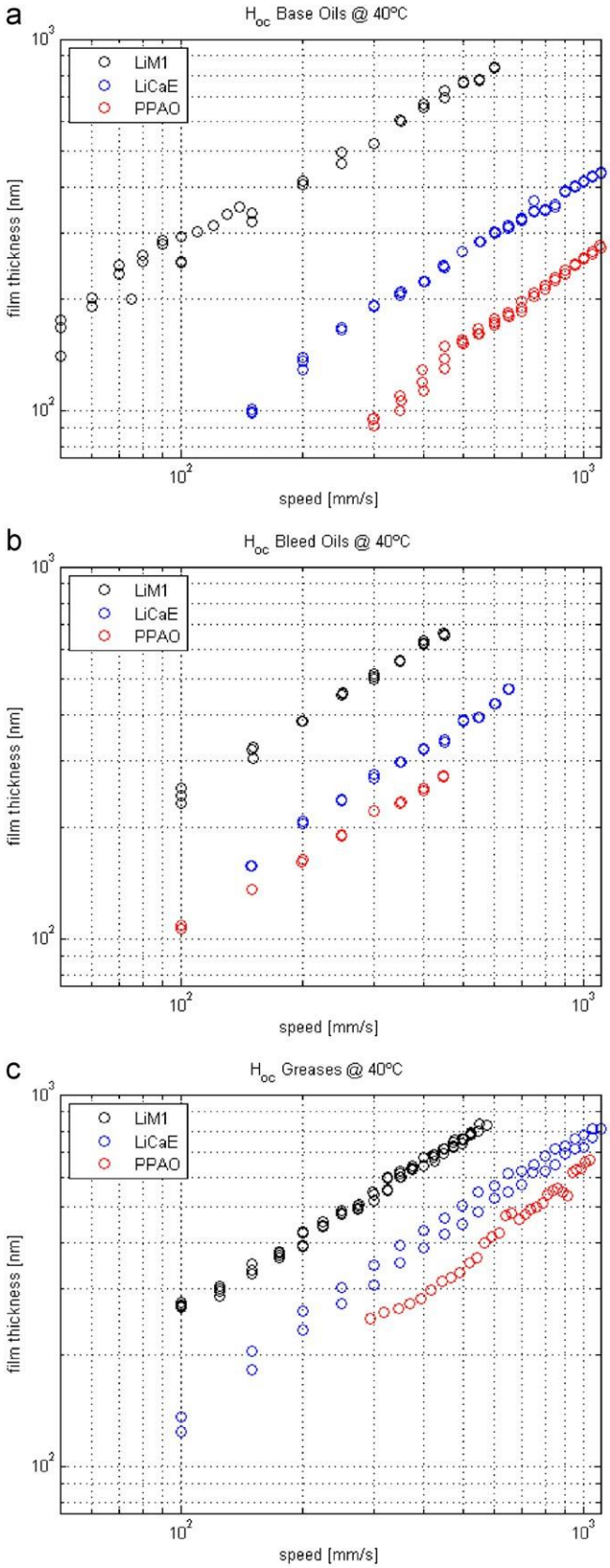

Fig. 3. Film thickness at 40 ¡C for all lubricants tested.

chamber and blowing hot air into this chamber. To ensure a homogeneous temperature (on the ball, disc, lubricant and chamber) three thermocouples were strategically positioned inside the chamber and the hot air was applied during at least 40 min before each measurement. The largest temperature oscillation measured was ± 1:5 ¡C during the 80 ¡C test. This variation did not generate significant differences in the film thickness values.

A different procedure was used for the oils, since a different arrangement had to be used. In this case the lubricant is heated in two different containers, which are connected through a tube. The small container, where the ball is partially submerged (up to the centre of the ball), was filled with around 10 ml of lubricant. The larger one, which supplies the small one through a pump, stores up to 200 ml. The base oil tests carried out with this configuration presented a slightly higher temperature oscillation, i.e., around ± 2:0 ¡C during the 80 ¡C test. In the case of the bleed oil, temperature oscillations were higher since there was not enough lubricant to fill both containers. In this case the highest temperature oscillation was around ± 2:9 ¡C during the 80 ¡C tests.

The temperature oscillations were considered in the calculations of all the parameters shown in the following results.

For each operating temperature the film thickness was measured from the lowest to the highest entrainment speed, with increments of 0.05 s, and then from the highest to the lowest entrainment speed. This procedure was repeated at least twice for each temperature and lubricant, giving a total of at least four measurements for each entrainment speed.

The scatter observed at the film thickness measurements was in the same order of magnitude as the differences observed between the tests with different SRR percentage (0 and 3%). Such scatter is mainly due to the temperature variations and the low stability of the machine at low entrainment speeds ¡ 0:1 m=s and low load 25.71 N.

All the tests were carried out under fully flooded lubrication in order to ensure that starvation effects played no part in determining the EHD film thickness. Therefore, the inlet lubricant supply, which has a large influence on film formation, is the same for greases, base and bleed oils.

3. Results and discussion

3.1. Viscosity measurements

The differences in kinematic viscosity between base and bleed oils (see Section 2.3) are due to the grease formulation. In fact, the thickener, the co-thickener and the additives may have a large affinity with the oil, bleed out together with it during the static bleed oil test and generate a bleed oil significantly different from the base oil. Furthermore, during the bleed oil test the thickener may pass through the mesh due to the imposed stress and temperature, thus thickening (or thinning) the bleed oil in comparison to the base oil. Therefore, the bleed oil may contain additives and thickener/co-thickener material, not presented in the base oil, and their amount in the bleed oil depends on grease formulation.

The bleeding process also depends on the geometry of the thickener structure, which interacts with the macromolecules of the oil and additives in a different way, accommodating or constraining them (see Fig. 2).

According to the manufacturer of the PPAO grease, the very high viscosity of the bleed oil is mainly due to the co-thickener, which is an elastomer with high affinity with the base oil and therefore bleeds out with it during the bleed process. The viscosities of the bleed oils of the Lithium greases (LiM1 and LiCaE) were similar to those of the base oils due to the greases formulations. These greases do not contain an elastomer as a co-thickener and the polymer molecules (viscosity improve additives), which is known to increase the viscosity, are much lower in concentration on these greases than in PPAO. It also may be

related to the thickener structure, which is more constraining in the case of the lithium greases, and therefore the bleeding of the macromolecules is more difficult.

The different compositions of the bleed oils have a significant impact on the film thickness.

3.2. Film thickness measurements

Fig. 3 presents the film thickness measured at 40 1C and different entrainment speeds, for the base oils (a), the bleed oils (b) and the greases (c). The results at 60 and 80 1C showed exactly the same trends and are not presented. In all cases, the film thickness increased with the entrainment speed at a rate of around $U^{0:67}$, as predicted by most of the film thickness equations. The lubricating greases and their base and bleed oils showed exactly the same trend, although they have significantly different properties (see Table 2), i.e. LiM1 (grease, base oil and bleed oil) always had the highest film thickness, PPAO always generated the lowest film thickness, while LiCaE appeared in between the other two.

Figs. 4–6 present the central film thickness measured for different entrainment speeds and temperatures for all greases, base oils and bleed oils. These figures show that each grease and its bleed oil generated a very similar central film thickness, whatever the grease considered. Vergne et al. [14,15] also found similar film thickness values between lithium mineral greases and their bleed oils. This observation is also in close agreement with the latest findings of the authors [22], where the predictions of the rolling bearing friction torque had better agreement with the corresponding measurements when bleed oil properties were used instead of base oil properties. Figs. 4–6 also show the calculated central film thickness for all base oils and bleed oils. The equations used to predict the central film thickness are presented in Section 3.3.

As shown in Figs. 4–6, the difference in central film thickness between bleed and base oils (or grease and base oil, since the bleed oil and the grease have similar film thickness values) is different for each lubricant. Such difference might be expressed by the relative film thickness increment Δh, defined by

$$\Delta h[\%] = \frac{h_{bleed} - h_{base}}{h_{base}} \times 100 \qquad (3)$$

The Δh is approximately constant for the whole range of the entrainment speeds, however some deviations are observed due to the scatter of the film thickness measurements. Fig. 7 shows the average values (and deviations) of the relative film thickness increment (Δh - Eq. (3)) for the different lubricants and temperatures.

Cann et al. [11] also studied the difference in central film thickness between greases and their base oils, and suggested that the relative film increment depends on the thickener type and its concentration, on the base oil viscosity and, above all, on the inlet lubricant supply. In the present work a temperature dependence was also put into evidence. The Δh increased with temperature, despite the fact that LiCaE shows lower Δh at 60 1C than at 40 1C. Fig. 7 also indicates that the relative film thickness increment (Δh) is very high in the case of the PPAO (between 80% and 180%, depending on the temperature) and significantly lower in the case of the LiM1 (between 10% and 25%). This figure also shows that all bleed oils (and consequently all the lubricating greases) had a significantly higher capability to build-up a lubricating film than the corresponding base oils, under the operating conditions considered. Such performance is even better at higher temperatures.

3.3. Pressure–viscosity coefficient

The film thickness inside an EHD contact is strongly dependent on the dynamic viscosity and on the pressure–viscosity coefficient of the lubricant. Under fully flooded conditions the influence of these

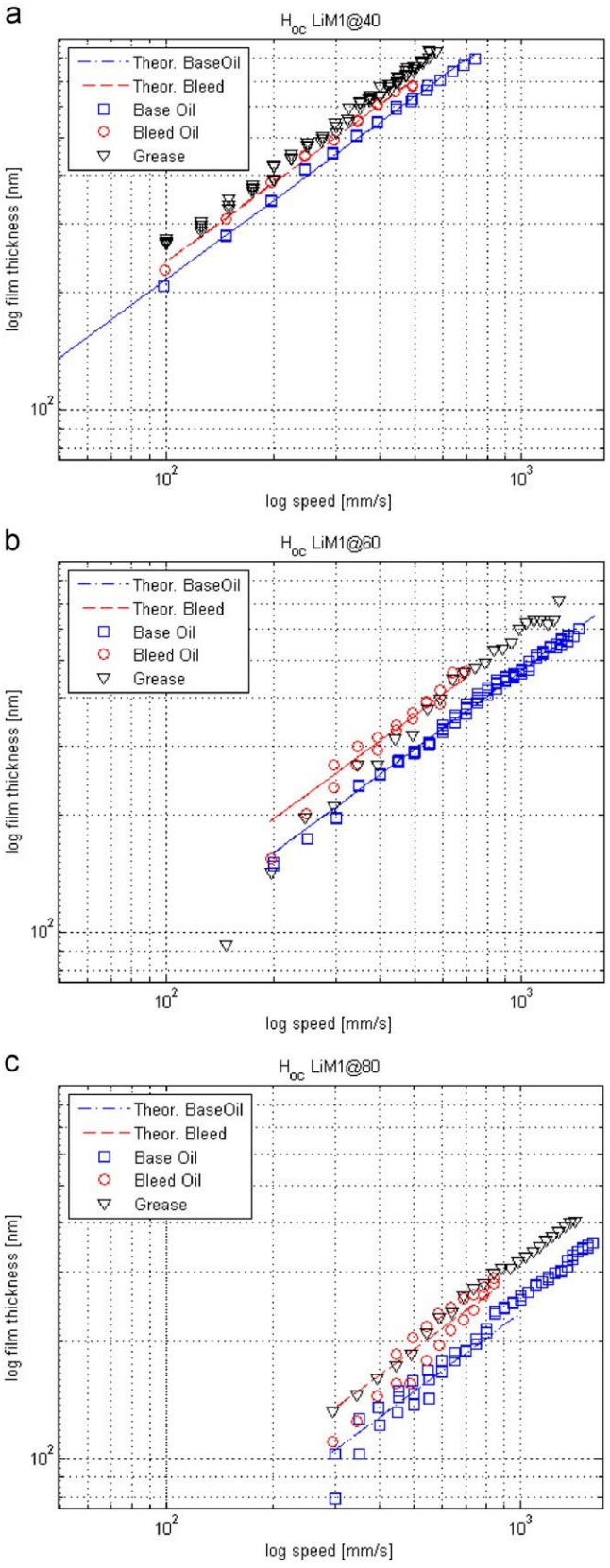

Fig. 4. Film thickness for LiM1 at different operating conditions: (a) 40 1C, (b) 60 1C and (c) 80 1C.

lubricant properties on the film thickness is well established, both experimentally and numerically. Several authors have proposed equations to predict the pressure–viscosity coefficient: Gold et al.

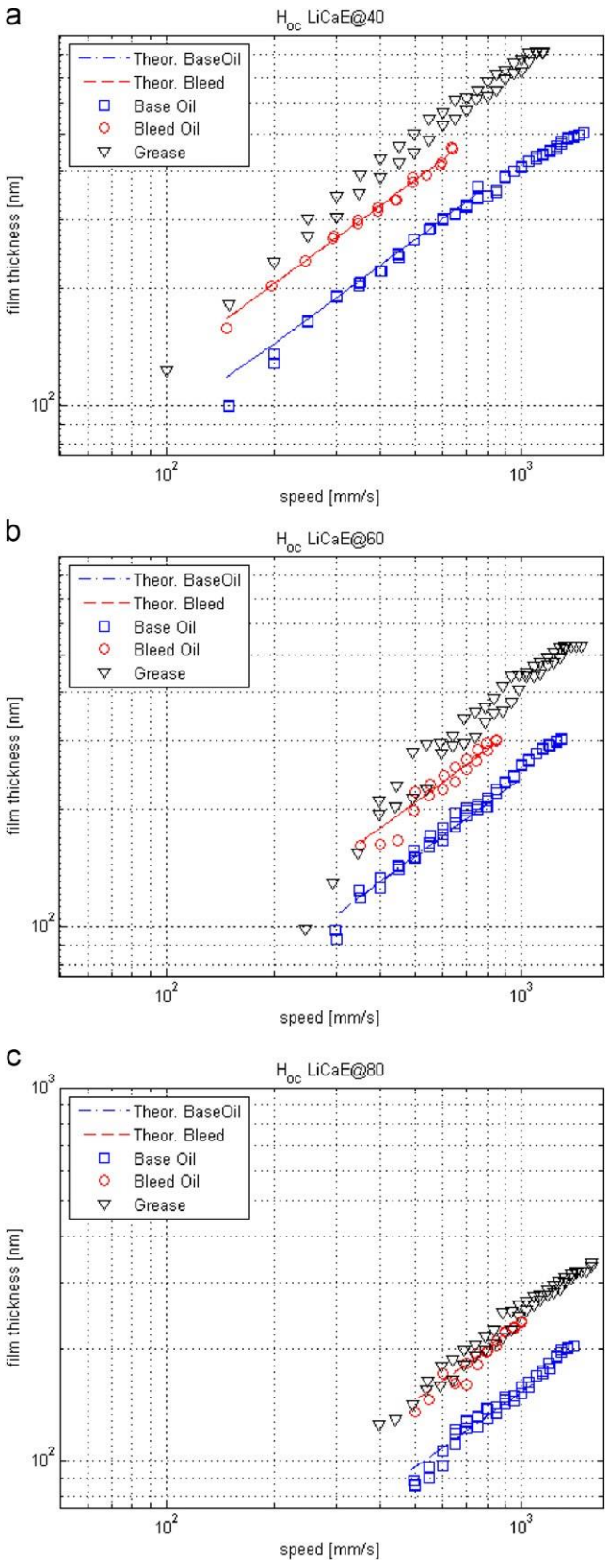

Fig. 5. Film thickness for LiCaE at different operating conditions: (a) 40 ºC, (b) 60 ºC and (c) 80 ºC.

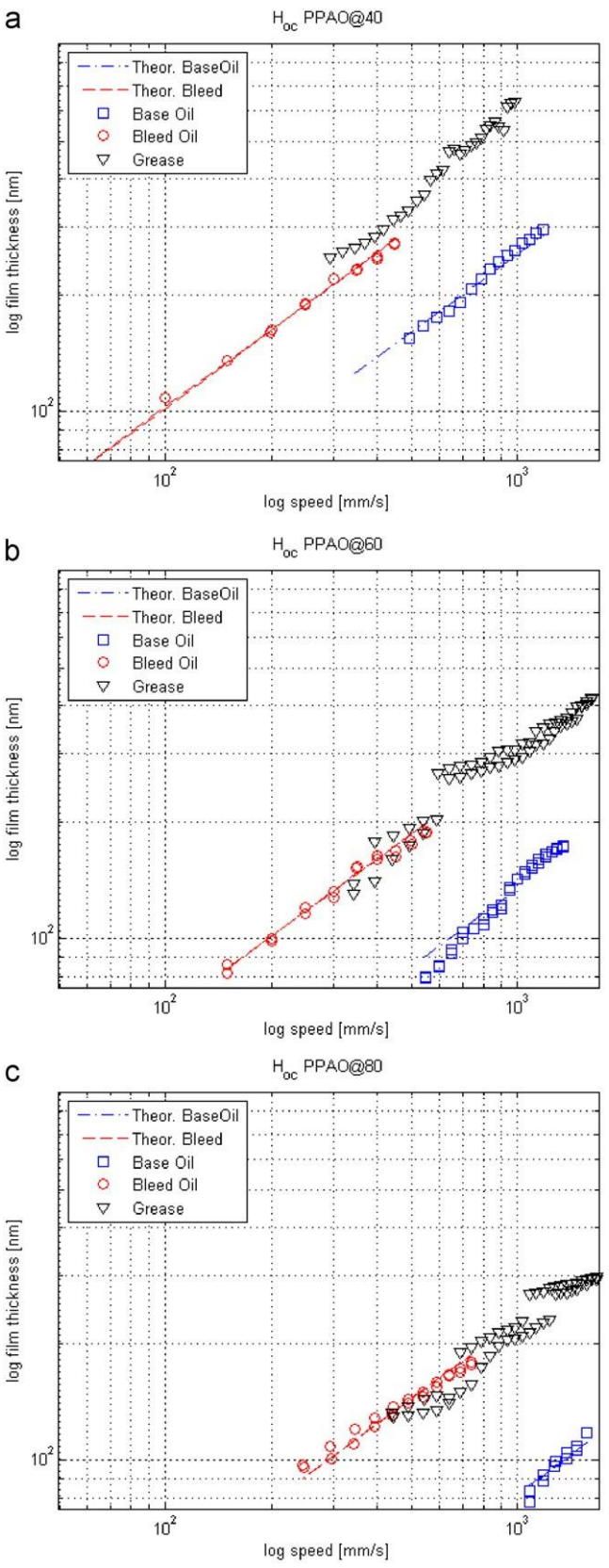

Fig. 6. Film thickness for PPAO at different operating conditions: (a) 40 ºC, (b) 60 ºC and (c) 80 ºC.

[23], So and Klaus [24], Fein [25], among others. The values predicted by these equations, however, show very large differences (Z 95%) whatever the base oil considered. This situation, together with the fact that high pressure rheological measurements are difficult and expensive, led to the extrapolation of the pressure–viscosity coefficient from film thickness measurements.

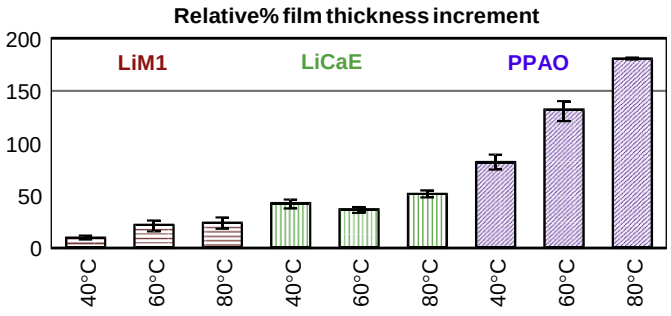

Fig. 7. Dh[%]– Relative percentage film thickness increment.

Table 3
Calculated pressure–viscosity coefficient.

a · [GPa^{-1}]	LiM1	LiE	PPAO
Base oil			
@ 40 [C	28.4	16.1	22.0
@ 60 [C	26.7	13.5	16.2
@ 80 [C	20.8	11.2	12.7
Bleed oil			
@ 40 [C	42.1	27.9	2.41
@ 60 [C	36.8	24.3	2.17
@ 80 [C	35.9	20.9	2.61

Recently, Van Leeuwen [26] compared accurate film thickness measurements with the values predicted by 11 different equations proposed in the literature, for two different base oils. The pressure–viscosity coefficient, a-, of one of the oils was known in advance. Van Leeuwen showed that the central film thickness equations proposed by Chittenden et al. [27] and Hamrock et al. [28] presented the best fitting (R^2 4 97%) for the lubricant with known a-value. Van Leeuwen also calculated the pressure–viscosity coefficient of the other base oil, using these equations and the film thickness measurements. A deviation of approximately 5% was observed.

The 'best' central film thickness equation, proposed by Van Leeuwen, was used to calculate the pressure–viscosity coefficients of base and bleed oils, using the corresponding film thickness measurements reported in Figs. 4–6 (see Appendix A). In the experiments, the contact geometry and the elastic properties of the ball and of the disc remained constant. Thus, according to Eq. (6), the differences in film thickness between grease, bleed oil and base oil can only be attributed to their different lubricant parameter *LP*, since the entrainment speeds and the loads are exactly the same. The *LP* is defined by the product of the lubricant dynamic viscosity Z by the pressure–viscosity coefficient a [23] and it is proportional to the lubricant film thickness in an EHD contact [29],

$$H_{0c} \propto LP = \eta^{0.67} \cdot \alpha^{0.53} \quad (4)$$

Table 3 presents the pressure–viscosity coefficients calculated for the base and bleed oils.

The base oil a– values are similar to other data published in the literature [30–32].

As observed for the dynamic viscosity, the pressure–viscosity coefficients of the base oils and of the bleed oils are significantly different from each other. The relative pressure–viscosity difference is defined by,

$$\Delta\alpha = \frac{\alpha_{bleed} - \alpha_{base}}{\alpha_{base}} \times 100 \quad (5)$$

At 40 [C two trends were observed: the pressure–viscosity coefficient of LiM1 and LiCaE bleed oils were 47% and 81% higher than the corresponding values for their base oils, while the pressure–viscosity coefficient of the PPAO bleed oil was 88% lower than its base oil. Such differences are also due to grease formulation. According to the manufacturer, the same elastomer that increased the PPAO bleed oil viscosity (see Table 2), in order to improve its film build up ability, reduces significantly its pressure–viscosity coefficient, in order to reduce the COF (see Table 3). Novak and Winer [33] measured, with a high-pressure viscometer, the pressure–viscosity coefficient of base oils blended with different polymers. The results showed that pressure–viscosity generally decreases with polymer molecule concentration. Novak et al. measured a reduction of 10%. Results published in the literature about the influence of lithium, calcium and additive package on the pressure–viscosity of the bleed oil are not clear. Pressure–viscosity measurements need to be performed in order to get a better understanding of the LiM1 and LiCaE behaviour.

4. Conclusions

The findings of this study can be summarized as follows:

- Different grease formulations, using different thickeners and base oils, produce bleed oils with significantly different rheological properties (viscosity and pressure–viscosity coefficient) and generate a very different film thickness;
- The pressure–viscosity coefficient of the greases' bleed oil can be calculated by correlating the film thickness measurements with the centre film thickness equation, if the bleed oil dynamic viscosity is taken into account;
- Lubricating greases and the corresponding bleed oils generate similar film thickness values, under fully flooded lubrication and for the same operating conditions;
- Grease and its bleed oil always generate a higher film thickness than the base oil, for the same operating conditions;
- Such difference is assigned to the thickener type and concentration, base oil viscosity, additive package, inlet contact supply and operating temperature;

These results suggest that the bleed oil plays an important role in grease lubrication and that the grease film thickness might be predicted if the viscosity and pressure–viscosity coefficient of the bleed oil are known.

According to Emeritus Professor Bo Jacobson, from Lund University in Sweden, a "controlled" oil bleed at low, ambient or high temperatures has already been reached. This implies not only the amount of oil bleed but also the properties of the released oil. (*private communication with Prof. Emeritus Bo Jacobson*, Lund University.)

Acknowledgements

The authors would like to thank the "Fundac-a-o para a Cie˜ncia e Tecnologia" (FCT) of the Portuguese Administration for support given to this study through the research project "Low friction, biodegradable and low-toxicity greases for rolling bearings" (ref. PTDC/EME-PME/72641/2006).

The authors would like to thank the Dr. Harold Bock from ROWE Mineralo¨lwerk Gmbh, in Bubenheim, Germany, for supplying the ester based grease LiE and Dr. Michael Kruse from AXEL

Christiernsson AB, Sweden, for supplying the polymer thickened grease PPAO.

Appendix A. Inlet shear heating

The Hamrock et al. centre film thickness equations are described as follows:

$$H_{oc} = 1.345 \cdot R_x \cdot U^{0.67} \cdot G^{0.53} \cdot W^{-0.067} \cdot C_0$$

$$U = \frac{\eta_0 \cdot (U_1 + U_2)}{2 \cdot R_x \cdot E^*}$$

$$W = \frac{2 \cdot F_N}{R_x^2 \cdot E^*}$$

$$G = 2 \cdot \alpha \cdot E^*$$

$$C_0 = 1 - 0.61 \cdot e^{(-0.752\,(R_x/R_y)^{0.64})} \quad (6)$$

Appendix B. List of symbols

H_{oc}	centre film thickness (mm)
$R_{x,y}$	equivalent curvature radius (mm)
U	speed parameter (–)
G	geometry parameter (–)
W	load parameter (–)
C_o	ellipticity influence (–)
U_1	ball speed (m/s)
U_2	disc speed (m/s)
En	equivalent Young modulus (Pa)
F_N	normal force (N)
a	pressure-viscosity coefficient (Pa^{-1})

References

[1] Lugt PM. A review on grease lubrication in rolling bearings. Tribology Transactions 2009;52(4):470–80.

[2] Booser E, Wilcock D. Minimum oil requirements of ball bearings. Lubrication Engineering 1953;9(June):156.

[3] Wikstro¨ m V, Ho¨ glund E. Starting and steady-state friction torque of grease-lubricated rolling element bearings at low temperatures—part II: correlation with less-complex test methods. Tribology Transactions 1996;39(3): 684–90.

[4] Cousseau T, Grac-a B, Campos A, Seabra J. Experimental measuring procedure for the friction torque in rolling bearings. Lubrication Science 2010;22(4):133–47.

[5] Espejel MG. Using a friction model as engineering tool. Evolution SKF 2006;6(2):27–30.

[6] Wilson A. Relative thickness of grease and oil films in rolling bearings. Proceedings of the Institution of Mechanical Engineers 1979;193:185–92.

[7] SY P. Experimental study of grease in elastohydrodynamic lubrication. ASME Transactions Journal of Lubrication Technology 1972;94 Ser F(1):27–34.

[8] Astro¨ m H, Isaksson O, Ho¨ glund E. Video recordings of an ehd point contact lubricated with grease. Tribology International 1991;24(3):179–84.

[9] Kaneta M, Ogata T, Takubo Y, Naka M. Effects of a thickener structure on grease elastohydrodynamic lubrication films. Proceedings of the Institution of Mechanical Engineers, Part J: Journal of Engineering Tribology 2000;214(4):327–36.

[10] Cann P, Spikes H. Film thickness measurements of lubricating greases under normally starved conditions. NLGI Spokesman 1992;56:21.

[11] Cann P, Williamson B, Coy R, Spikes H. Behaviour of greases in elastohydrodynamic contacts. Journal of Physics D: Applied Physics 1992;25(1A): A124–32.

[12] Scarlett N. Use of grease in rolling bearings. Proceedings of the Institution of Mechanical Engineers 1967;182(PART 3A):585–93.

[13] Cousseau T, Grac-a B, Campos A, Seabra J. Friction and wear in thrust ball bearings lubricated with biodegradable greases. Proceedings of the Institution of Mechanical Engineers, Part J: Journal of Engineering Tribology 2011;225(7):627–39, http://dx.doi.org/10.1177/1350650110397261 /arXiv:http://pij.sagepub.com/content/225/7/627.full.pdfþ htmlS.

[14] Couronne´ I, Vergne P, Mazuyer D, Truong-Dinh N, Girodin D. Effects of grease composition and structure on film thickness in rolling contact. Tribology Transactions 2003;46:31–6.

[15] Couronne´ I, Vergne P, Mazuyer D, Truong-Dinh N, Girodin D. Nature and properties of the lubricating phase in grease lubricated contact. Tribology Transactions 2003;46:37–43.

[16] Bjo¨rling M, Larsson R, Marklund P, Kassfeldt E. Ehl friction mapping: the influence of lubricant, roughness, speed and slide to roll ratio. Proceedings of the Institution of Mechanical Engineers, Part J: Journal of Engineering Tribology 2011;225:671–81.

[17] Johnston GJ, Wayte R, Spikes HA. The measurement and study of very thin lubricant films in concentrated contacts. STLE Tribology Transaction 1991;34:187–94.

[18] Guangteng G, Cann P, Olver AV, Spikes HA. Lubricant film thickness in rough surface, mixed elastohydrodynamic contact. Journal of Tribology 2000;122:65–76.

[19] Cann PM, Spikes HA, Hutchinson J. The development of a spacer layer imaging method (slim) for mapping elastohydrodynamic contacts. Tribology Transactions 1996;39:915–21.

[20] Gustafsson L, Hoglund E, Marklund O. Measuring lubricant film thickness with image analysis. Proceedings of the IMechE, Part J: Journal of Engineering Tribology 1994;208:199–205.

[21] Hartl M, Krupka I, Liska M. Differential colorimetry: tool for evaluation of chromatic interference patterns. Optical Engineering 1997;36(9):2384–91, http://dx.doi.org/10.1117/1.601415 URL /http://link.aip.org/link/?JOE/36/2384/1S.

[22] Cousseau T, Graea BM, Campos AV, Seabra JH. In fluence of grease rheology on thrust ball bearings friction torque. Tribology International 2012;46(1):106–13, http://dx.doi.org/10.1016/j.triboint.2011.06.010 URL / http://www.sciencedirect.com/science/article/pii/S0301679X11001691S.

[23] Gold P, Schmidt A, Dicke H, Loos J, Assmann C. Viscosity-pressure-temperature behaviour of mineral and synthetic oils. Journal of Synthetic Lubrication 2001;18(1):51–79.

[24] So B, Klaus E. Viscosity-pressure characteristis of lubricating oils. ASLE Transactions 1980;23:409–21.

[25] Fein R. Liquid lubricants. In: Friction, lubrication, and wear technology, ASM handbook, vol. 18. ASM International, Metals Park, OH; 1992.

[26] van Leeuwen H. The determination of the pressure-viscosity coefficient of a lubricant through an accurate film thickness formula and accurate film thickness measurements. Proceedings of the Institution of Mechanical Engineers, Part J: Journal of Engineering Tribology 2009;223:1143–63.

[27] Chittenden RJ, Dowson D, Dunn JF, Taylor CM. A theoretical analysis of the isothermal elastohydrodynamic lubrication of concentrated contacts, Part I: direction of lubricant entrainment coincident with the major axis of the hertzian contact ellipse. Proceedings of the Royal Society London A397(1813); 1985. p. 245–69.

[28] Hamrock BJ, Schmid SR, Jacobson B. Fundamentals of fluid film lubrication.2nd edition Basel: Dekker; 2004.

[29] Hamrock BJ, Dowson D. Ball bearing lubrication, the elastohydrodynamics of elliptical contacts. John Wiley & Sons; 1981.

[30] Roelands C. Correlational aspects of the viscosity-temperature-pressure relationship of lubricating oils. PhD thesis. Delft University of Technology; 1966.

[31] Fang N, Chang L, Johnson G, Webster M, Jackson A. An experimental/theoretical approach to modelling the viscous behaviour of liquid lubricants in elastohydrodynamic lubrication contacts. Proceedings of the Institution of Mechanical Engineers, Part J: Journal of Engineering Tribology 2001;215(4): 311–8.

[32] Hong H-S, Bair S. Film-forming tendencies of some base fluids and viscosity modifiers. Journal of Synthetic Lubrication 1999;16(3):233–45, http://dx.doi.org/10.1002/jsl.3000160304.

[33] Novak J, Winer W. Some measurements of high pressure lubricant rheology. ASME Journal of Lubrication Technology 1986;90:580–91.